Int J Adv Manuf Technol (2001) 17:508–515

The International Journal of Advanced Manufacturing Technology

A Hole-Plate Artifact Design for the Volumetric Error Calibration of CMM

E. S. Lee[1] and M. Burdekin[2]

[1] Department of Mechanical Engineering, Chungbuk National University, Choungju, South Korea; [2]Department of Mechanical Engineering, UMIST, Manchester, UK

To measure the volumetric error of coordinate measuring machines (CMMs), a hole-plate artifact method was studied. Example designs of the hole-plate are shown using titanium and ceramic materials. The deflection by its own weight of the designed hole-plate is analysed using the finite element method. The hole distances moved by the deflection are shown in different hole-plate set-up cases, for vertical and horizontal positions. The influence of inside hole roundness as a measuring standard is also studied. Eccentric errors for different hole roundness are simulated. The hole-plate set-up errors are also discussed. A method for obtaining the parametric errors of a CMM is shown using the hole-plate as a measuring artifact for CMM positioning error. In addition, a method for measuring 2D and 3D length errors using the hole-plate data is introduced.

Keywords: Coordinate measuring machine (CMM); FEM (finite element method); Hole plate; Hole roundness; Parametric error; Three-dimensional length error; Volumetric error

1. Introduction

To measure the positioning error of machine tools, plate type test bodies, artifacts, ball/hole plates [1,2] or cone plates [3] have been developed. All the plate artifacts used to measure the errors of a coordinate measuring machine (CMM, Fig. 1) require the calibration centre distances of the ball/hole/cone to be known [4] Using the ball/cone plate, 3D measurement is possible but the hole plate method uses only 2D measurements. The minimum number of touch points for determining a ball centre is four compared with three points needed for a hole plate. In the case of cone plate, only one touch point is required to determine the cone centre. However, there will be some uncertainties of contact with the cone. The cone plate

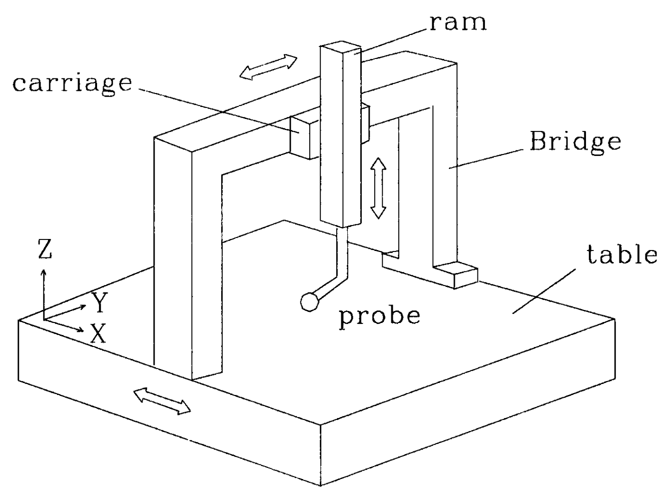

Fig. 1. Moving-bridge-type CMM.

will be useful for checking manually operated CMMs. In the ball outside type (with ball stem), bending of the plate results in changes of the ball centre distance, which is not serious in a hole/cone plate or a ball inside type (ball centres placed on the same plane with the plate), as shown in Fig. 2. The bending could be due to thermal expansion or other external forces such as plate weight and clamping. There are some advantages in using the ball plate, but ball height calibration is difficult; however, it is not required in the case of hole plates. Also, the exposed ball surfaces are susceptible to damage during transit. As for hole plate, hole manufacturing, squareness with respect to the plate face, and hole roundness, will influence the measuring accuracy. For a ball plate, standard high-precision balls are readily available from specialist ball manufacturers.

In this study, a hole-plate method is used as a transfer standard for measuring the volumetric error of CMMs. Examples of the hole-plate design are shown using titanium and ceramic materials. The deflection by its own weight of the designed hole-plate is analysed using the finite element method. The movement of the hole centre caused by the deflection is shown in different hole-plate set-up cases, for

Correspondence and offprint requests to: Dr Eung-Suk Lee, Department of Mechanical Engineering, Chungbuk National University, Cheongju, Chungbuk, 361–763, South Korea. E-mail: eungsuk@cbucc.chungbuk.ac.kr

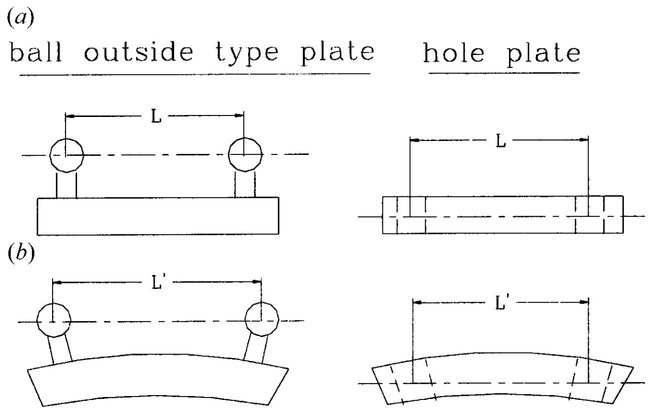

Fig. 2. The influence of bending in the plate centre. (*a*) Before expansion. (*b*) After expansion.

vertical and horizontal positions. We also discuss measuring the hole in the plate, and hole inside roundness errors. The influence of the hole roundness error for the eccentric centre position of the hole is simulated. The hole plate set-up errors are also discussed. Using the hole-plate measurement data, we developed a method to analyse machine parametric errors. Two-dimensional length error measurements using the hole-plate artifact are shown. A method for measuring 3D length error by combining a series of 2D data using a hole plate is also proposed. The results and the method of this paper will be useful for hole-plate designers and users.

2. Hole-Plate Design

British Standard [BS-7172] recommends at least five different points to determine a circle, although three points determine a circle mathematically. In this case, the measured hole diameters should be large enough for the CMM probe to touch at five different points. However, such large hole diameters result in a large hole plate. To remove the thermal distortion of the hole plate, the best plates are designed without a hole insert, but use a different material. Usually, it is not easy to obtain high-precision manufacturing of hole roundness in the hole plate. There are some commercial inserts in which the hole roundness is adequate, such as a polished bearing bush. It is more practical to use such a hole insert instead of direct manufacturing in the plate. The general steps for hole-plate design are proposed as follows;

1. CMM positioning error measuring scheme:
   Parametric errors.
   2D and 3D length error.
2. Determination of hole-plate shape and size for CMM measuring volume.
3. Number of holes in a line on the hole plate and the size of hole.
4. Layout drawing of the hole plate.
5. Deflection analysis of the hole plate.
6. Hole-plate material and manufacturing method selection.
7. Hole inside roundness and squareness error verification for the manufacturing method.
8. Hole-plate calibration method.

Figure 3 shows examples of a hole-plate design using titanium and ceramic materials in order to reduce the thermal effect. Both types are set horizontally with three supports and designed to be used with an electronic level, for roll error measurement, inside the plate. The inside material of the Type A plate is removed to reduce its weight, and is designed to be used with a hole insert. The inside of the hole in the ceramic hole plate, Type B, is polished to improve the roundness. The thicknesses of the two plates are 30 mm, and they can be set vertically without other support. The weight of the hole plates was limited for easy transport by one person.

2.1 Deflection Analysis of the Hole Plate

Usually, the hole plate will be designed with some inside part removed to reduce its weight. Figure 4 shows three different types of hole plate, with rectangular meshes for FEM analysis. Because of the symmetry of a hole-plate design, as shown in Fig. 3, only half of the plate was analysed. To avoid complex FEM mesh generation, the areas of the measuring holes were ignored. However, the mass of holes was removed in the applied load calculation as shown in Fig. 6. Practically, the plate will be set in a horizontal or vertical position on the table. In this study, the two cases of distributed load by the weight of hole plate itself were assumed, as shown in Fig. 5. For the boundary condition, the *X*-, *Y*- and *Z*-direction con-

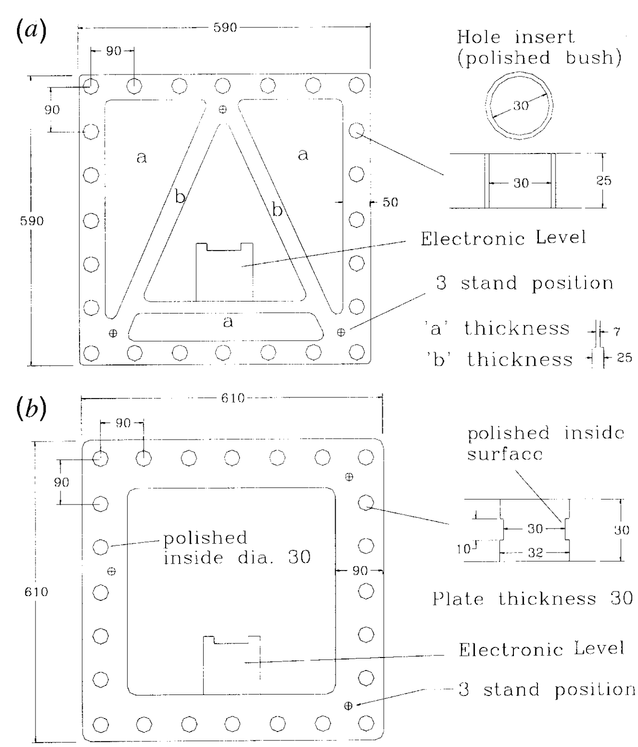

Fig. 3. Examples of hole-plate design. (*a*) Type A, titanium, weight = 12.5 kg. (*b*) Type B, ceramic, weight = 12 kg. Unit: mm.

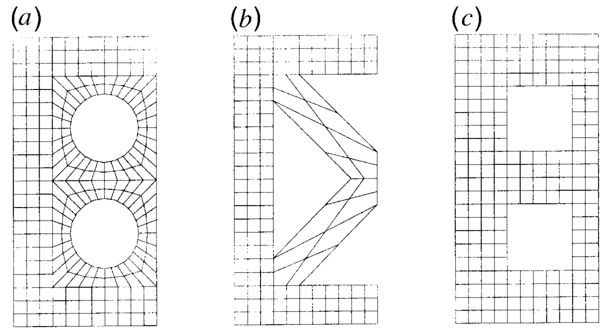

Fig. 4. Mesh generation of different inside types of hole plates for FEM analysis. (*a*) 4-circles. (*b*) 4-triangles. (*c*) 4-rectanles.

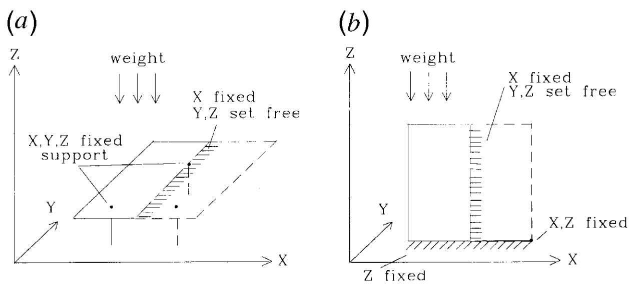

Fig. 5. Two cases of applied loads in using the plate and boundary conditions. (*a*) Horizontal set-up. (*b*) Vertical set-up.

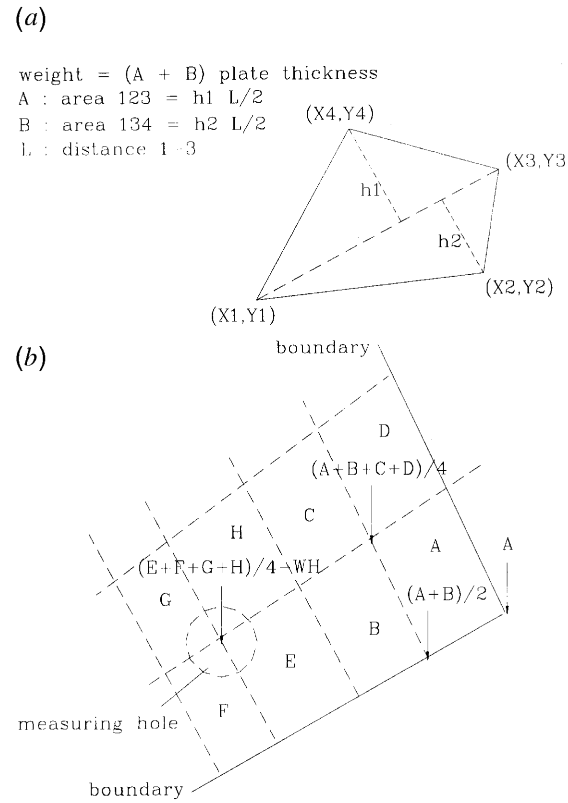

Fig. 6. Calculation of (*a*) the weight of a general rectangular area, and (*b*) the weight in each node position, for the distributed load. WH, hole weight for the area; A, B, C, D, E, F, G, H, weight in each element.

straints were set free in all elements, except for the 3-support positions on the vertical centre-line of the plate, and the bottom side in the case of the vertical set-up. Each weight of the general rectangular element was calculated as shown in Fig. 6(*a*). Applied loads at different nodes were assumed, as shown in Fig. 6(*b*), by the weights of surrounding elements. If the node position was the same as the position of the measuring hole, the weight for the hole area was removed.

2.1.1 Horizontal Set-up Case

The hole-plate material was assumed to be titanium (Young's modulus: 110 400 N mm^{-2}, density: $4.434 \times 10^3\ \text{kg m}^{-3}$, Poisson's ratio: 0.34 at the ambient temperature). Table 1 shows the vertical deflection at the measuring holes, with respect to the plate surface, by FEM analysis. In this calculation, an external load by the plate's own weight using three horizontal supports, was applied. The total weight of the plate was calculated as approximately 13 kg, and the three support positions were considered to be the same, for the three types of hole late. The positions of the measuring holes are given in Fig. 7, as node points. The results shown in Table 1 indicate that the maximum deflection point in the plate is at hole 4 in types A and B, and at hole 6 in type C. Figure 8 shows the magnified deflection in the *Z*-direction using the results of Table 1. In practice, the deflection in the *Z*-direction will not be serious. In this study, using the *Z*-deflection and two directional bending angles, which is the method used in FEM plane stress analysis, the hole position changes in the *X*, *Y*-direction were calculated. In the case of a small deflection of a beam, two assumptions are usually made [5]:

Table 1. Deflection of holes in the *Z*-direction by FEM analysis in the half plate for different hole-plate types, distributed load by the plate's own weight in the horizontal set-up case. Titanium plate size: $590 \times 590\ \text{mm}^2$, thickness = 20 (24 holes, dia. 30 mm). Deflection unit [μm].

Plate type W (kg) Hole number	*A*, 4 circles = 100 mm 13.390	*B*, 4 triangles $125 \times 250\ \text{mm}^2$ 13.213	*C*, 4 rectangles $125 \times 125\ \text{mm}^2$ 13.213
1	0.617	4.726	−1.175
2	0.722	11.981	−0.177
3	4.677	10.843	2.737
4	8.243	15.108	6.248
5	7.627	13.555	7.033
6	6.866	11.606	7.134
7	5.776	9.280	6.411
8	4.010	6.228	4.722
9	1.619	2.561	1.727
10	−0.820	−1.216	−1.200
11	−0.970	−0.284	−0.456
12	−0.713	0.790	0.806
13	−0.535	1.257	1.267
MD	9.424	16.727	7.863

W, total weight of the plate; MD, maximum deflection in the plate

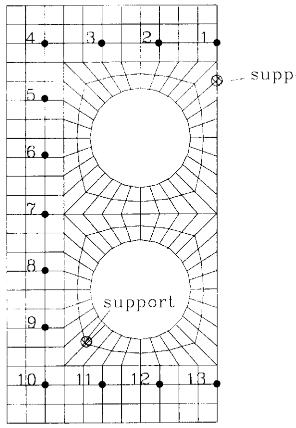

Fig. 7. Measuring hole positions in the case of an inside-circle-type plate.

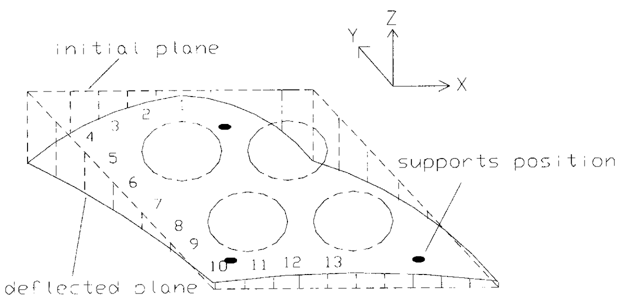

Fig. 8. Deflection feature in the *Z*-direction of the hole plate supported at three positions in the case of a horizontal set-up.

1. The length of the centre-line from the clamped point will not change after bending.
2. The bent centre-line of the beam will be circular.

Figure 9 shows the calculation method for deflection in the *X*,*Y*-direction. From the *Z*-deflection (w) and bending angle in the *X*-direction (Qy), the curvature of the beam centre (radius R in triangle COP), is expressed as follows:

$$R = \frac{w}{2\sin^2(Qy/2)} \tag{1}$$

Therefore, the deflection in the *X*-direction (v) is,

$$\begin{aligned} v &= L - \frac{w}{\mathrm{Tan}(Qy/2)} \\ &= 2\pi R \frac{Qy}{2\pi} - \frac{w}{\tan(Qy/2)} \\ &= \frac{w}{\sin(Qy/2)} \left[\frac{Qy}{2\sin(Qy/2)} - \cos(Qy/2)\right] \end{aligned} \tag{2}$$

The deflection in the *Y*-direction can be calculated using the same equation using the bending angle in the *Y*-direction (Qx). Table 2 shows the calculated deflections in the *X*-, *Y*- and *Z*-directions at each hole position. From this result, the maximum deflection in the *X*,*Y*-direction is at the same position (hole 4) as the maximum *Z*-deflection and it is very small, being less then 0.001 μm in the *Y*-direction.

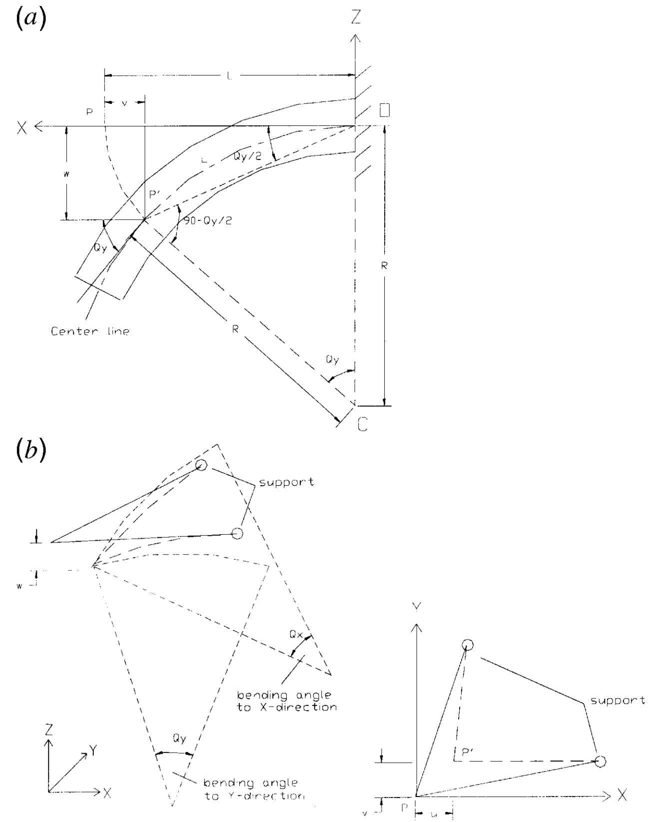

Fig. 9. The calculation method in the *X*, *Y*-direction deflection using (*a*) the deflection in the *Z*-direction, and (*b*) the *X*, *Y*-direction bending angles.

Table 2. Deflection of holes in the *X*-, *Y*- and *Z*-directions, by the hole-plate weight in the horizontal set-up case (hole-plate with 4-circles type inside, radius = 100 mm).

Hole number	Deflection [μm]	
	X	Y
1	0.0000000	0.0683960
2	0.0001020	0.0692970
3	−0.0009026	0.0653590
4	−0.0003073	0.0585500
5	0.0056225	0.0559140
6	0.0084318	0.0506120
7	0.0079255	0.0421380
8	0.0113430	0.0320970
*9	0.0100980	0.0188450
10	0.0074510	0.0042146
11	0.0034401	0.0021994
12	0.0020329	0.0013284
13	0.0000000	0.0030252

2.1.2 Vertical Set-up Case

Table 3 shows the deflections in the case of a vertical hole-plate set-up, for an inside circle type plate. The deflection was due to compression by the hole-plate weight, and the magnified deflection feature was drawn in Fig. 10. In this result, the

Table 3. Deflection of holes in the *X*-, *Y*-directions by FEM analysis in vertical hole-plate set-up, by compression load due to the hole-plate's own weight (4-circles inside type, radius = 100 mm).

Hole number	Deflection [μm]		
	X	*Y*	*Z*
1	0.0000000	0.0000016	0.6173800
2	0.0000142	0.0000040	1.7225000
3	0.0000600	0.0000088	4.6773000
*4	0.0001102	0.0000182	8.2430000
5	0.0000958	0.0000181	7.6277000
6	0.0000743	0.0000225	6.8665000
7	0.0000489	0.0000288	5.7761000
8	0.0000219	0.0000316	4.0102000
9	0.0000053	0.0000152	1.6192000
10	–0.0000012	–0.0000070	–0.8207000
11	0.0000004	–0.0000068	–0.9708100
12	0.0000008	0.0000042	–0.7136900
13	0.0000000	–0.0000029	–0.5358800

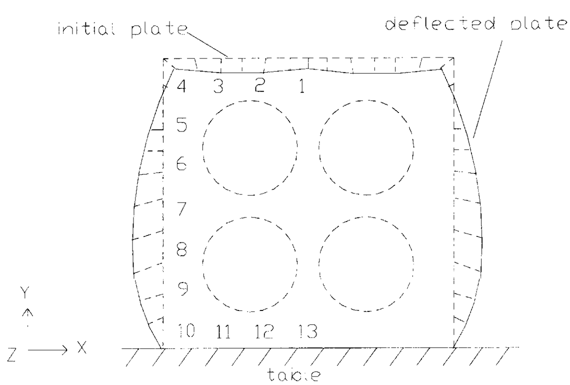

Fig. 10. Deflection in the *X*,*Y*-direction by the plate's own weight in the vertical set-up case.

maximum deflection is at hole 9, being less then 0.02 μm in the *X*-direction, which is also very small when using the plate for the calibration of industrial machine tools.

2.2 Hole Roundness Effect

The inside of the manufactured hole will include roundness errors, which are not uniformly distributed or periodical. However, hole roundness may not seriously influence the least-squares circle centre. We studied the hole roundness effect on the eccentricity of the least-squares circle centre, using a roundness error simulation method. The hole roundness error was simulated to be (roundness band)/2 with respect to the nominal radius. Measuring points for uniformly or non-uniformly spaced angles were considered, as shown in Fig. 11(*a*). Figure 11(*b*) shows an example of the least-squares circle determined by the simulated error, with 7 points with uniform angle division. The eccentricity was defined as the distance from the nominal centre to the least-squares circle centre as follows:

$$Eccentricity = \sqrt{(Xc^2 + Yc^2)} \quad (3)$$

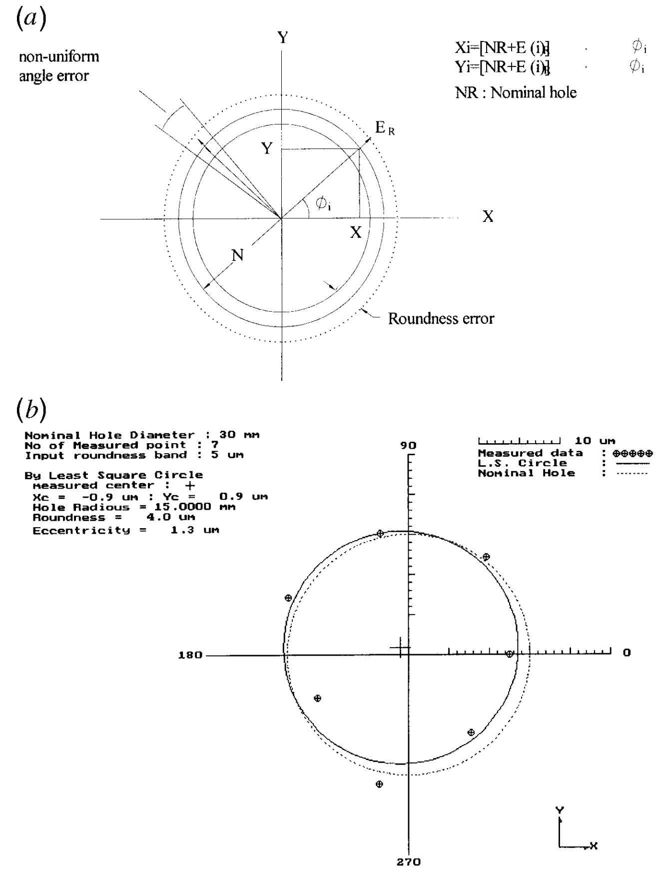

Fig. 11. (*a*) Roundness error simulation as E_R = (roundness band)/2, with non-uniform spaced points. (*b*) An example of the calculated least-squares circle using the simulated hole roundness error.

where *Xc* and *Yc* are eccentric *X*-, and *Y*-coordinates of the least-squares circle. Figure 12 shows the influence of different roundness errors on the eccentricity of the least-squares centre, using 50 times randomly simulated roundness errors. In this calculation, it was assumed that the CMM probe touches at 7 or 14 uniformly spaced points around the inside of the hole. From Fig. 12(*a*), it is seen that the eccentricity of the hole is less then 1 μm from a perfect hole centre for up to a 3 μm hole roundness error. It is assumed that the manufacture of a hole with a 3 μm roundness is not very difficult. The eccentricity when using 14 measuring points is smaller than when using 7 points. The calculation results for non-uniform angularly spaced measuring points around the hole were very similar to those for the uniformly spaced data.

3. Hole-Plate Set-Up Errors

The hole may include some roundness and squareness errors with respect to the plate face. However, if the measuring height is the same as for the calibration, those errors can be minimised. There are four types of hole-plate set-up errors, as shown in Fig. 13. The horizontal set-up error is due to the different lengths of the horizontal supports or to uneveness of the table. Case C of vertical set-up errors is due to the vertical

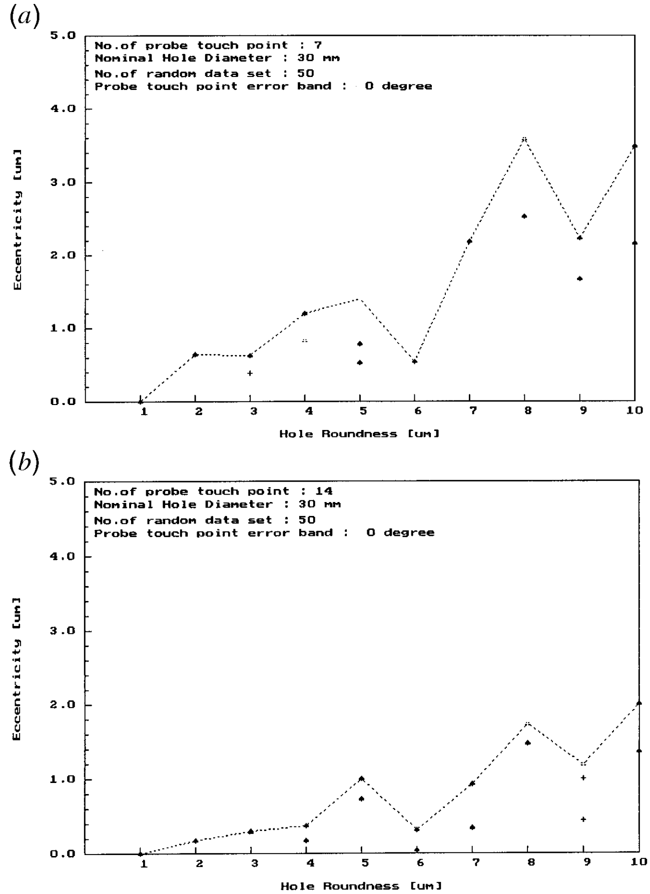

Fig. 12. Hole roundness effect on the calculated eccentricity of the least-squares circle centre, with assumed uniformly spaced measuring points, (*a*) with 7 data points, (*b*) with 14 data points.

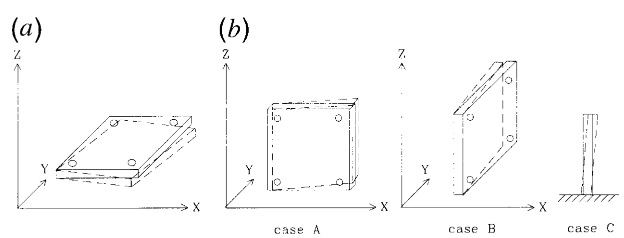

Fig. 13. Hole-plate set-up errors, (*a*) horizontal, (*b*) vertical.

supports uneveness of the table. The set-up errors will influence the hole distances by the inclined angle of the plate. To minimise the effects of set-up errors, calibration is required in different horizontal set-up positions. Though the compensation of set-up errors is possible, it is inevitable that the CMM probe touch points will be changed with respect to the nominal measuring height, owing to the set-up errors.

3.1 Data Transformation into Calibration Coordinate

Measured hole data includes set-up errors, which are due to the rotation of the axis of the plate with respect to the calibration axis, in the vertical set-up cases. To compare with the calibration coordinates, the coordinate transform, as shown in Fig. 14, is essential. Therefore, excluding the hole-plate inclined angle (ϕ_{17}), real measured coordinates at hole i are,

$$Xm(i) = \sqrt{(Xi^2 + Yi^2)} \cdot \cos(\phi_i - \phi_{17})$$

$$Ym(i) = \sqrt{(Xi^2 + Yi^2)} \cdot \sin(\phi_i - \phi_{17}) \quad (4)$$

where (Xi, Yi) are measured coordinates including the set-up angle. Therefore, the two components of position errors at hole i are,

$$e(X,i) = Xm(i) - Xc(i)$$

$$e(Y,i) = Ym(i) - Yc(i) \quad (5)$$

where $[Xc(i), Yc(i)]$ are calibration coordinates at hole i.

3.2 Compensation of Set-up Errors

The set-up errors, which are due to the different lengths of the horizontal support, vertical support set-up error, or uneveness of the table, will cause a cosine error in the hole distance. If these errors are serious, they must be compensated for using measured set-up angles, as mentioned previously. Therefore, the real distance L will be $L' \cos(\phi)$, where ϕ = set-up angle in the axis, L' = hole distance including cosine error. For example, if the difference in the height of the supports is 0.1 mm in 590 mm distance, the error between two centre holes will be 0.008 μm ($590 - 590 \times \sqrt{(590^2 - 0.1^2)}/590$).

4. Volumetric Error Verification

4.1 Hole-Plate Data Measurement

The hole-plate data will be measured by a CMM for six different set-up cases, as shown in Fig. 15(*a*). In cases 3 and 4 or 5 and 6, the distance between the two set-up positions (*XD* or *YD*) will be chosen to be twice the CMM probe length. The hole-plate vertical set-up angles with respect to the CMM table are measured in set-up cases 3,4,5, and 6, for the roll error calculation, as shown in Fig. 15(*b*). Measured holes data include set-up errors which are due to the inclined angle with respect to the calibration axis in the vertical set-up cases.

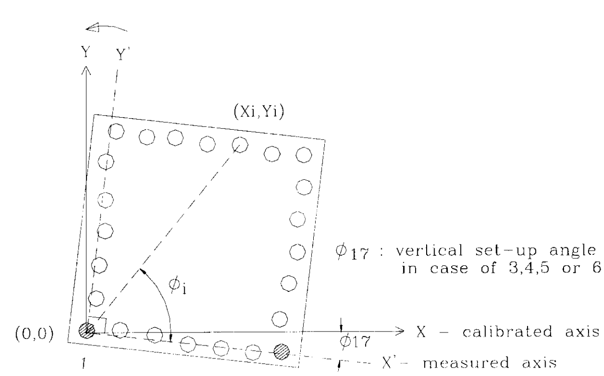

Fig. 14. Axis rotation of measured data to the calibration coordinate.

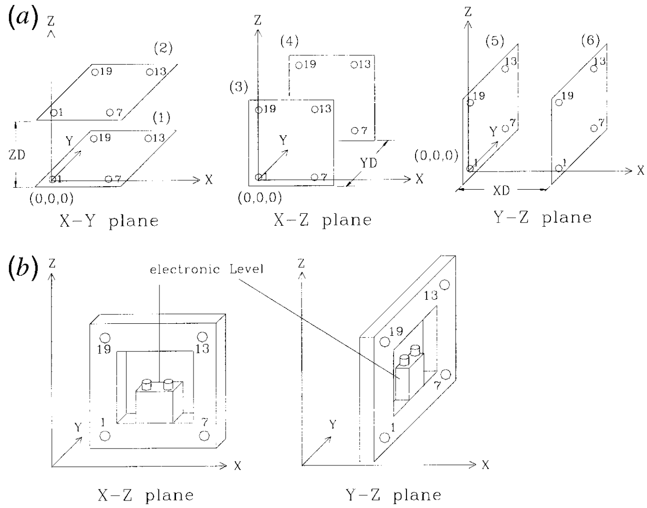

Fig. 15. Hole-plate (24 holes, 7 × 7) set-up cases and measurement of the hole-plate set-up angle for roll error calculation. (*a*) Six set-up cases in 3 planes on a CMM table. (*b*) Vertical set-up angle measurement.

Therefore, to compare with the calibration coordinates, a coordinate transform will be required.

4.2 Parametric Error Analysis

It is possible to verify the 21 parametric error components of CMM using the hole-plate data measured in the six set-up case, as shown in Fig. 15. Figures 16–18 show the method for angular error measurement, of yaw, pitch, and roll in the *Y*-axis (*Ez*(*Y*), *Ex*(*Y*), and *Ey*(*Y*)) using the hole line data. In the case of roll error measurement, the hole-plate vertical tilting angles (ϕ_5 and ϕ_6 in set-up cases 5 and 6) are included owing to the CMM table flatness error in the *Z*-direction for the two set-up cases. Therefore, the influence of the tilting angle at Y_i on the *Z*-direction error for the calculation of *Y*-roll error, *HT*(*i*) should be compensated for. The hole-plate tilting angle

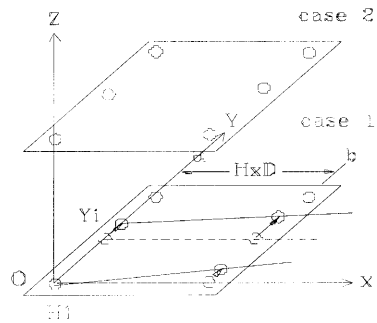

$$Ez(Yi) = \frac{[e_y(i,b) - e_y(i,a)] - [e_y(1,b) - e_y(1,a)]}{HxD}$$

Fig. 17. *Y*-yaw error measurement and calculation using hole data $e_y(i,a)$, e_y (*i,b*; *Y*-direction hole errors at hole *i* in hole lines *a* and *b*.

also effects the *X*-direction error for the *Z*-roll measurement to the same degree, *HT*(*i*).

The position error can be measured easily using the hole error data in the same direction as the hole line. Straightness error can also be measured using the orthogonal error data from the hole line. The squareness error is calculated from the best-fit lines of two straightness errors in the same plane. The *X-Y* squareness, *Sxy* can be measured from the hole-plate set-up case 1, for *Sxz* from case 3 and for *Syz* from case 5.

4.3 Three-Dimensional Length Error

From the hole-plate data, the error vectors (*ex*, *ey*) for each hole in the six set-up cases, a 2D length error measurement is possible. Using data measured from any two holes in the orthogonal direction, a 2D length error *E*(*i*, *j*) between two holes *i* and *j* can be calculated, as shown in Fig. 19. Measuring the 3D length error is also possible by using the 2D hole distance data for the six set-up cases. Figure 20 shows the 3D measuring data points with the 3D error vector, that were combined using the six hole-plate set-up cases. At each data

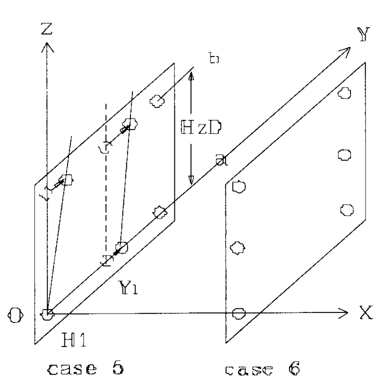

$$Ex(Yi) = \frac{[e_y(i,b) - e_y(i,a)] - [e_y(1,b) - e_y(1,a)]}{HzD}$$

Fig. 16. *Y*-pitch error measurement and calculation using hole data $e_y(i, a)$, e_y (*i,b*); *Y*-direction hole errors at hole *i* in hole lines *a* and *b*.

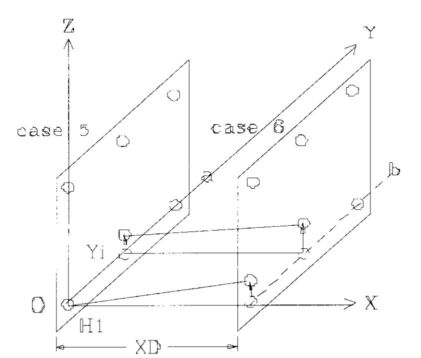

$$Ey(Yi) = \frac{[e_z(i,b) - HT(i) - e_z(i,a)] - [e_z(1,b) - ez(1,a)]}{XD}$$

$$\text{where} \quad HT(i) = Yi \cdot Tan(\phi_6 - \phi_5)$$

Fig. 18. *Y*-roll error measurement and calculation using hole data e_z (*i,a*), e_z (*i,b*); *Z*-direction hole errors at hole *i* in hole lines *a* and *b*.

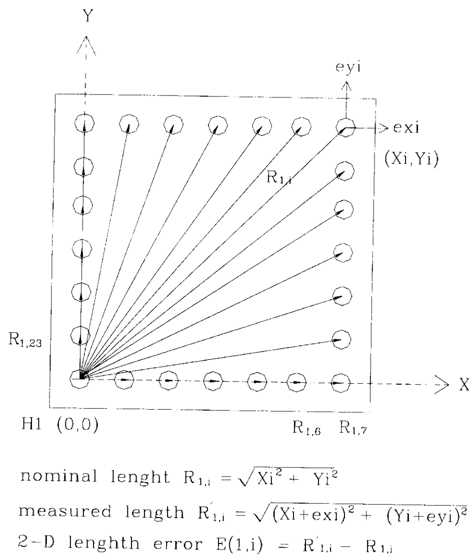

Fig. 19. Two-dimensional error, $E(l,i)$ calculation with respect to hole 1.

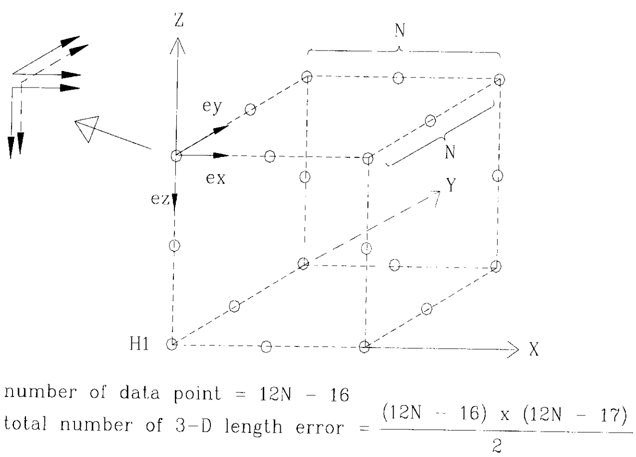

Fig. 20. Cubic measuring points by the combination of the six hole-plate set-up cases for 3D length error measurement.

point, two sets of 3 component error vectors can be obtained, which arise from the three hole-plate set-up data. Using any two hole error vectors (*ex*, *ey*, *ez*), a 3D length error calculation is possible.

5. Conclusions

We have shown the possible use of a hole-plate artifact method for measuring the volumetric accuracy and 21 parametric error components of a CMM. The deflection analysis using a finite element method for the hole-plate design shows that hole position movement caused by the weight of the plate was very small (less than 0.02 μm in the hole positioning axis, i.e. the *X*, *Y*-direction). This study shows that the deflection effects by the plate weight are negligible when using the hole plate as a positional accuracy measuring device for industrial NC machine tools. The deflections in the *Z*-direction, i.e. the vertical axis to the hole plate, were greater than 8 μm which will be significant in the case of 3D artifacts such as ball plates. The hole-plate calibration technique is also important for minimising the influence of hole manufacturing errors, e.g. hole roundness. An analytic technique for the simulated hole roundness error showed that the influence of the hole roundness error was not very significant for determining the hole centre.

References

1. British Standard BS 6808, Parts 1, 2 and 3: Coordinate Measuring Machines, 1989.
2. E. Trapet and F. Waldele, “A reference object based method to determine the parametric error components of coordinate measuring machine and machine tools”, Measurement, 9(1), 1991.
3. J. S. Lim, K. C. Nam and M. S. Chung, “A two-dimensional test body for calibration of coordinate measuring machines”, Precision Engineering, 10(3), July 1988.
4. E. S. Lee, “Volumetric error calibration of CNC-machine and coordinate measuring machines using artifact method”, PhD thesis, Manufacturing division, UMIST, 1993.
5. S. Timoshenko, and Woinowsky-Kreiger, Theory of Plate and Shell, 2nd edn, McGraw-Hill, 1959.

Nomenclature

$ey(i, a)$	error vector at hole *i* along the *Y*-axis using hole plate *a*
E_R	roundness error
$E(i, j)$	2D error vector at hole *ij*
$HT(i)$	roll error compensation factor in hole *i*
$Ex(Y)$, $Ez(Y)$, $Ey(Y)$	pitch, yaw and roll error in the *Y*-axis
HxD, HyD, HzD	distance between two hole lines
L	beam length
R	curvature of beam centre
Qy	bending angle to the *X*-direction
Qx	bending angle to the *Y*-direction
Xc, *Yc*	eccentricity in *X*-, *Y*-coordinates
XD, *YD*, *ZD*	distances between the two hole plates in the *X*-, *Y*- and *Z*-direction
Xi, *Yi*, *Zi*	coordinates of hole i
w	deflection in the *Z*-direction
v	deflection in the *X*-direction
ϕ	divided angle in a hole, hole-plate vertical tilting angle